WATER STRUCTURE IN VITAMIN B_{12} COENZYME CRYSTALS

I. Analysis of the Neutron and X-ray Solvent Densities

HUGH SAVAGE

Center for Chemical Physics, National Bureau of Standards, Gaithersburg, Maryland 20899 and Laboratory of Molecular Biology, National Institute of Arthritis, Diabetes, and Digestive and Kidney Diseases, National Institutes of Health, Bethesda, Maryland 20892

ABSTRACT The disordered solvent distribution in crystals of vitamin B_{12} coenzyme was examined using the methods of high-resolution neutron and x-ray diffraction. One set of neutron (0.95 Å) and two sets of x-ray (0.94 and 1.1 Å) data were collected and the resulting models were extensively refined using least-squares and Fourier syntheses. The solvent regions were analyzed in two stages: first, main sites were assigned to the well defined regions of solvent density and refined using least squares; second, continuous sites were assigned representing the more disordered diffuse and elongated regions of solvent density. During the analysis an acetone molecule was also located. Water networks were formulated from the assigned sites in the above models and also from those assigned in the original structure determination (Lenhert, 1968), using criteria that included hydrogen bonding (derived from small crystal hydrates), van der Waals contact distances, side-chain disorder, water molecule orientations, and the presence or absence of foreign solvent. The well established networks extend throughout all the solvent regions of the crystal with interesting orientational arrangements of the individual waters around both polar and apolar groups of the coenzyme molecule. The networks were seen to be consistent among each of the four models in terms of occupying relatively similar positions. However, the occupancy values of the individual networks varied between the models; some networks were clearly visible in one but attenuated in another. The specific details of the water structure (bonding geometries, short-range nonbonded contacts, orientations of the waters, polar and apolar interactions, etc.) are described in the following paper.

INTRODUCTION

In biological systems, water is known to be an important component. Its existence is crucial for the structural integrity and functioning of these multicomponent systems. The hydration layer around biomolecules is currently described, on a qualitative level, in terms of deviations from the bulk solvent properties, for example, restricted movements, stronger binding, preferential binding sites. At the microscopic end of the scale, little is known about how the individual water molecules in the solvent may be structured in terms of their instantaneous static arrangements (relative positions and mutual orientations), and possible mobilities. To address some of these problems the method of single crystal diffraction is concentrated on here in the analysis of the solvent structure around the biomolecule: vitamin B_{12} coenzyme.

To obtain a complete description of the possible water structure, the positions of both the oxygens and hydrogens are required. Unfortunately, the structural information gained from most x-ray analyses of biomolecules (e.g., proteins) furnish only the possible water oxygen positions with any reliability. This is because the hydrogen atom has a relatively low scattering cross section for x-rays (1 electron) compared with other elements present in biological structures. The most reliable method for the detection of hydrogen atoms is by neutron diffraction, since the coherent scattering cross section is comparable to that of the other atoms.

Protein crystals often contain between 40–60% solvent and, in principle, offer extensive systems in which water-water and water-biomolecular interactions can be examined: work in this area has been discussed and reviewed by Edsall and McKenzie (1983, 1978), Finney et al. (1985, 1982), Finney (1978, 1977), Cooke and Kuntz (1974), and Kuntz and Kauzmann (1973). Ideally we would like to examine water structure around proteins using neutron diffraction data to atomic resolution (~1.0 Å or below). However, the availability of such data for these systems is very limited. Few proteins have been analyzed to below 1.5 Å resolution: crambin (Teeter and Kossiakoff, 1984) and lysozyme (Mason et al., 1984) to 1.4 Å. In addition, there are also problems with the extent of solvent disorder and its

Dr. Savage's present address is the Medical Foundation of Buffalo, Inc., 73 High Street, Buffalo, New York 14203.

TABLE I
DIFFRACTION DATA OF SPACEGROUP $P2_12_12_1$

	Neutron	X-ray1	X-ray2	1968x-ray
Range of data (in angstroms)	0.95	1.10	0.94	~1.2
Wavelength (in angstroms)	1.67	1.5418	1.5418	1.5418
Temperature (degrees centigrade)	6 (±1)	~4	~4	~21
Cell parameters (in angstroms)				
a	27.849	27.701	27.809	27.93
b	21.736	21.608	21.712	21.73
c	15.368	15.351	15.333	15.34
Number of $F_o > 0.0$	5,994	4,390	~6,100	3,068
Number of $F_o > 3\sigma(F_o)$	5,601	4,152	5,621	*
Refinement methods	L. Sq.‡ Dif. F.‖	L. Sq. Dif. F.	L. Sq. Dif. F.	Dl. Syn§ Dif. F.
Crystallographic *R* factor	0.085	0.088	0.136	0.132

*not reported
‡L. Sq., Least squares refinement,
§Dl. Syn, Differential synthesis refinement,
‖Dif. F., Difference Fourier syntheses.

possible interpretation in large hydrate crystals (Savage and Wlodawer, 1986).

The intermediate-sized biomolecular system of vitamin B_{12} coenzyme (dry M. W. = 1,580) promised to be a good candidate for a solvent analysis since (*a*) it is large enough to present a sizeable solvent interface, (*b*) it contains between 60–70 water molecules per unit cell of the crystal, (*c*) it contains a variety of groups of biological interest that interact with the solvent, (*d*) it is well ordered in the crystal, and (*e*) very high-resolution neutron and x-ray data to 0.9 Å were obtainable from which the hydrogen positions of both the coenzyme B_{12} and water molecules could be located.

This paper is the first of two describing the results of the solvent investigation in coenzyme crystals. Here, details of the examination of the individual regions of solvent density and the formulation of solvent networks are given, while in the second paper, structural details of the networks, water-polar and water-apolar interactions, and possible movements of the water molecules are described. In a separate analysis, the method of Monte Carlo computer simulation was applied to predict the water structure within the coenzyme crystal (Vovelle et al., 1985). Several different models were used to describe the water-coenzyme and water-water interactions and the derived solvent networks compared with the experimental ones obtained here.

BACKGROUND AND PREVIOUS WORK

In this section we briefly outline the details of (*a*) the experimental data collection and refinement, (*b*) the molecular structure, and (*c*) solvent distribution within the crystals of vitamin B_{12} coenzyme. The full experimental details, along with the geometries of the coenzyme molecule, are presented in a separate publication (Savage et al., 1986).

Data Collection and Refinement

A set of high-resolution neutron data to 0.95 Å was collected from one crystal grown in D_2O, using a four-circle diffractometer installed on a thermal neutron beam tube of the nuclear reactor at the Institut Laue-Langevin, Grenoble, France. The crystal with an approximate volume of 6 mm^3 was maintained at a temperature of 6(±1)°C. To improve the x-ray data obtained from the original structure determination (Lenhert and Hodgkin, 1961; Lenhert, 1968) and to assist in the interpretation of the solvent in the neutron model, two sets of x-ray diffraction data were collected at a temperature of ~4°C on a four-circle diffractometer. The first set (x-ray1) to a resolution of 1.1 Å using one crystal, and the second (x-ray2) to a higher resolution of 0.94 Å, for which two crystals were used.

A summary of the crystal data and the refinement of the three coenzyme models is given in Table I. The structure was refined using the methods of partially blocked full matrix least-squares and difference Fourier syntheses. Anisotropic thermal parameters were included for each of the coenzyme atoms and isotropic values for the individual solvent sites. The three coenzyme models along with the one obtained from the original structural analysis (Lenhert, 1968) are referred to in Table II. In three of the four models a molecule of acetone (used in the crystallization procedure) with a partial occupancy was located. When present, this molecule divides the water distributions

TABLE II
THE THREE COENZYME MODELS

Name	Resolution	*R* factor	Solvent	Acetone presence
1968x-ray	~1.2Å	0.132	H_2O	Not located
X-ray1	1.1	0.088	D_2O	yes
X-ray2	0.94	0.136	D_2O	yes
Neutron	0.95	0.085	D_2O	yes

within the crystal (see below) into two separate regions, a pocket and a channel. In addition to this, one of the side chains (the *c* side chain) of the coenzyme B_{12} molecule was found to be disordered (next section), consequently influencing the surrounding water structure.

Coenzyme B_{12} Molecule and Side-Chain Disorder

The coenzyme B_{12} molecule (see Fig. 1 *a*) comprises a central corrin nucleus to which the following side groups are attached: 3 acetamides, 3 propionamides, 1 propionic acid, and 8 methyl residues. A nucleotide (containing a benzimidazole base) and a nucleoside are also attached to the ring nucleus by direct links to the cobalt atom. The nucleotide is also bonded to the propionic group through the phosphate.

The acetamide *c* side chain was found to be disordered in the neutron model with the ND_2 group (N40) being the most variable part of the chain (see Fig. 2). The occupancies assigned for alternative nitrogen positions (N40 and N640) in the different models are given in Table III.

The disorder appears to be somewhat complicated in that the carbonyl oxygen O39 remains relatively stationary, while the amide N40 group occupies several alternate positions. Fig. 2 shows three of the possible conformations for this side chain in the neutron model. The two extreme positions for the amide, N40 and N640, are ~1.8 Å apart. The reason why the carbonyl oxygen does not move very

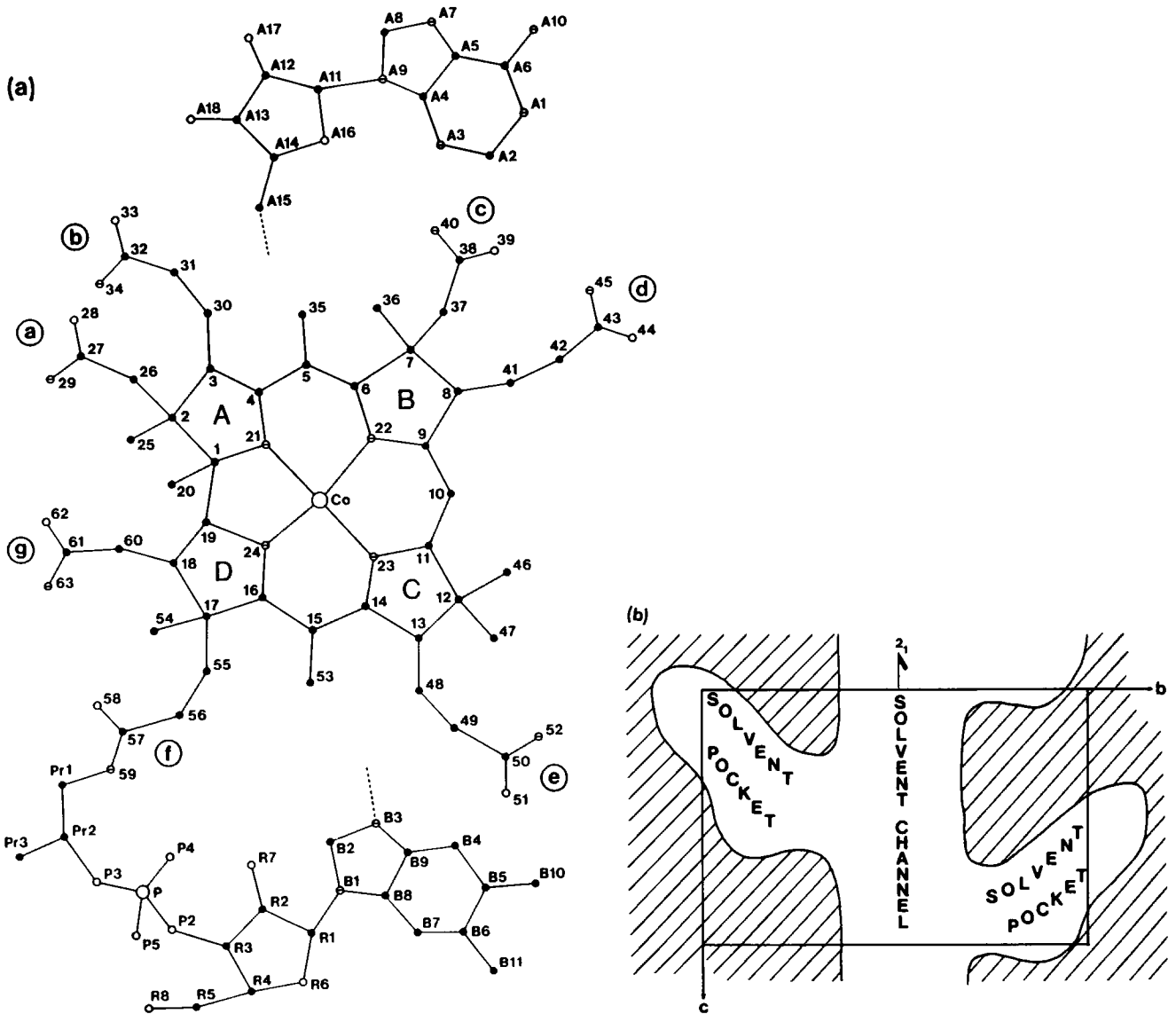

FIGURE 1 (*a*) Arrangement of the atoms in the coenzyme B_{12} molecule. The chemical formula is $C_{72}H_{100}O_{17}N_{18}PCo$ and the undeuterated dry M.W. is 1,580. The side chains are labeled by circled letters. The atom code is: filled circles, C (*large*), H (*small*); open circles, O (*small*), Co and P (*large*); open circles with horizontal line, N. (*b*) Distribution of the solvent regions within the unit cell of the coenzyme B_{12} crystal, viewed down the *a* axis. Shaded areas represent the coenzyme molecules.

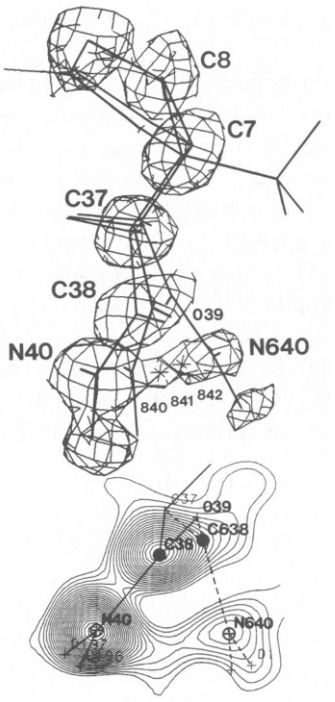

FIGURE 2 Neutron density over the disordered *c* side chain: partial difference $F_o - F_c$ Fourier synthesis omitting the *c* side chain and the B pyrrole ring from the phasing calculation. (*Top*) Cage (Frodo) density representation; contour level = 0.08×10^{-12} cm. Three positions of the side chain are included: N40, N840, and N640. (*Bottom*) Difference density over the C38, C638, N40, and N640 sites. Contour interval = 0.03×10^{-12} cm.

much can be related to the local nonbonded contacts of O39 to a nearby methyl group (CPr3) of a symmetry related molecule. If O39 moved as a result of a rotation about the C37-C38 bond, the new position would approach the adjacent methyl group to within 3.0 Å, less than the expected van der Waals contact distance of ~3.5 Å. The neutron densities over the atoms of the side chain are elongated in certain directions (Fig. 2 *a*) and the disorder can be accounted for by small changes in the positions and torsion angles of the atoms in both the side chain (maintaining its planarity) and the pyrrole ring (Fig. 2 *a*).

Solvent Distribution

Within each unit cell of the crystal, the solvent region is separated into two main unconnected cavities situated between the layers of the coenzyme molecules. Viewed down the *a* axis of the unit cell (Fig. 1 *b*), each cavity can be seen to be composed of (*a*) a central channel region, forming a continuous path throughout the crystal, parallel to the twofold screw axes along *c* at $x = 1/4$, $y = 1/4$ for one cavity, and $x = 3/4$, $y = 0$ for the other. (*b*) Two pocket regions, which lead off from the central channel into blind alleys at intervals related to the symmetry of the twofold screw axis along the channel. The asymmetric unit comprises one half of the channel region and one of the pocket regions.

The density of the wet crystals grown in D_2O solution was measured by flotation in an acetone-bromoethanol mixture. The measured density was found to be 1.38(1) g-cm^3 at room temperature, compared with the measured density of 1.36(1) g-cm^3 obtained in the original structure determination, where the crystals were grown in H_2O. From these measurements, between 16 and 18 water molecules per asymmetric unit were estimated to be present, thus each cavity (2 asymmetric units) was expected to contain 32–36 waters.

TABLE III
OCCUPANCIES FOR ALTERNATIVE NITROGEN POSITIONS

Model	N40	N640	Temperature
X-ray1	1.00	—	4°C
X-ray2	1.00	—	4°C
Neutron	0.74	0.26	6°C
1968x-ray	—	1.00	21°C

METHODS: STRATEGY OF THE SOLVENT ANALYSIS

Use of All Available Models

The analysis of the disordered solvent structure from just the neutron data alone appeared in the early stages to be too complicated. Three main problems arose. First, the determination of the chemical identities of solvent peaks that were further than 2.5 Å from the coenzyme polar atoms (>3.4 Å from the nonpolar atoms) was often unclear. This was due to the relative similarity of the neutron scattering lengths of oxygen and deuterium atoms ($O = 0.58 \times 10^{-12}$ cm, $D = 0.667 \times 10^{-12}$ cm). Second, many of the solvent sites appeared to be disordered with possible alternative positions for both the oxygen and deuterium atoms of each water molecule. In addition, many of the disordered sites were either partially or completely overlapped, making their interpretation, in terms of chemical identity and occupancy, very difficult.

To alleviate these problems, the solvent oxygen positions from the three x-ray models were used to identify the neutron oxygen sites. However, the x-ray solvent sites were themselves disordered with several sites of the order of 1 Å, or less, apart. With the theoretical addition of two deuterium sites for each disordered oxygen site, some of the peaks in the neutron model were thus expected to be unresolved.

A further difficulty was also seen to occur, in terms of the individual water site occupancies: individual sites had different occupancy values in the separate models. For example, in the neutron model the water sites associated with the two main positions of the disordered *c* side chain (see above) were assigned occupancies of 0.6 and 0.4, but in the x-ray1 and x-ray2 models they were assigned values of 0.9 and 0.1, while in the 1968x-ray model they were 0.0 and 1.0. Although the different occupancies for solvent sites in the four models appeared at the outset to be a problem, it turned out that the different values provided a reasonable indicator for the acceptance of peaks as possible solvent sites that were at or near the noise level in one of the models, but well above in another. Thus, a comparative analysis of the solvent regions in all four models was undertaken.

Solvent Refinement

The detailed analysis and refinement of the solvent regions in the neutron, x-ray1 and x-ray2 models involved the calculation of a series of difference syntheses based on the fully refined parameters obtained from the

least-squares refinement of the coenzyme molecule. Initially, all the solvent was omitted from the phasing calculations and as various parts of these regions were identified, they were included in the model. Further difference syntheses were computed with various combinations of the refined solvent sites (for instance, one of the assigned water networks), included in the phasing. The solvent peaks located in the difference maps were generally accepted to represent solvent positions if (*a*) they were well above the noise level of the map, (*b*) there was evidence of their existence in one or more of the other solvent models (especially for low peaks near the noise level [occupancies ~0.1]), and (*c*) they made sensible H-bonded and nonbonded contacts to surrounding sites (see criteria used for the formulation of water networks).

All the assigned solvent sites were included in the least-squares refinement, but only the parameters of the sites that did not overlap with distances of <0.9 Å between them were allowed to vary. No restraints were applied, but future refinements will have to incorporate them for the disordered groups (covalent bond lengths and angles, orientations, etc.).

During the early analysis it became evident from the solvent density distributions that the sites could be roughly divided into two categories:

(*a*) "Main" sites representing the most ordered sites. These sites were usually H-bonded to one or more of the coenzyme polar groups and located in well defined regions of solvent density. This group can be further divided into "major" and "minor" sites, depending on their occupancy values: "major" sites having occupancies >0.3 and "minor" sites with relatively low occupancies, <0.3.

(*b*) "Continuous" sites representing disordered sites associated with the continuous regions of solvent density situated around and between the ordered "main" sites. These sites were usually seen to have low occupancies of <0.3.

The continuous regions were modeled by including sites spaced at the resolution of the expected temperature factors (the mean displacement value, usually 0.2–0.5 Å) for that region, obtained from the refined major and minor sites. The interpretation and refinement of the solvent regions proceeded in two stages. First, the better defined regions of solvent density were analyzed and "main" ("major" and "minor") sites assigned. Then, from these sites possible (alternative) water networks were formulated. Second, with the ordered sites located, the more disordered regions of solvent density became more apparent and "continuous" sites were assigned. These latter sites represent alternative solvent positions that may correspond in part to local mobilities of the individual waters in the time averaged solvent density.

Formulation of Water Networks

Water networks were formulated from the assigned solvent sites using the following criteria:

(*a*) Hydrogen bonds were initially assigned between solvent oxygen sites and either polar atoms of the coenzyme molecule or other solvent oxygen sites for distances between the limits of 2.5 and 3.3 Å, that is, the accepted limits of hydrogen bonding for a water molecule in small crystal hydrates (Ferraris and Franchini-Angela, 1972; Chiari and Ferraris, 1982).

(*b*) Water sites were accepted where the X...O(W)...Y angles subtended at water oxygens were within the limits of 69° and 148° found in small crystal hydrates (Chiari and Ferraris, 1982). However, angles down to 65° (involving longer O...O,N distances, >3.0 Å), were observed for several of the main water sites, and the minimum acceptable angle was subsequently reduced to this value.

(*c*) Where mutually exclusive sites occurred (<2.5 Å apart) alternative networks were selected for each of the conflicting sites.

(*d*) Where possible, networks were formulated in which the oxygen sites had similar occupancies.

In addition to these four criteria, it became apparent that the following factors also had to be taken into consideration:

(*e*) The disorder of the *c* side chain between two main positions.

(*f*) The presence or absence of the acetone molecule was the most crucial factor in determining which of the solvent sites belonged to a particular network. The solvent networks could be divided into two groups, those that included the acetone molecule and those that did not.

(*g*) The nonbonded D...D distances between the water molecules in the neutron model were inspected to ensure that none of the water deuterium contacts were closer than 2.0 Å — the lower limit of the expected van der Waals contact distance.

ANALYSIS OF THE SOLVENT REGIONS: MAIN SITES

The analysis of the solvent density in the x-ray1, x-ray2, and neutron models is discussed here, and comparisons are made between each of these and also with the 1968x-ray model. Fig. 3 shows a summary of the main (*a*) neutron and (*b*) electron (x-ray2) solvent densities, projected onto the *bc* plane of the unit cell. The code used in the following figures for the atomic symbols is given in the legend of Fig 1 *a*. Few differences were observed between the relative positions of the "main" solvent sites (when present) located in the different models, but significant variations were observed among the models with respect to the occupancy values of individual sites (sometimes as large as 0.8).

Below, the analysis of one particular region of solvent density (211/212) is described in detail to illustrate the inherent complexities: the remaining regions are summarized mentioning only the main features.

Pocket Region

On the first impression, five of the major sites in the x-ray1, x-ray2, and neutron models (211, 212, 213, 216, and 217) appeared to be fully occupied, since very little solvent density was initially observed in their immediate surroundings and they were also hydrogen bonded to eight of the polar coenzyme groups. However, when the regions around each of these individual waters were examined in more detail, several alternative sites could be placed that were <2.5 Å away (mutually exclusive sites).

211/212 Region. This region essentially corresponds to the end of the pocket region where the disordered C-side chain is situated (Figs. 2 and 3). Fig. 4 shows (*a*) neutron and (*b*) x-ray2 sections through the solvent density surrounding the disordered N40 group (the main alternative N640 position is not shown but is situated ~1.8 Å behind the N40 position). In the x-ray1 and x-ray2 models two "major" sites 211 and 212 were observed. In addition to these sites, three small peaks (601, 603, and 604) were also present just above the noise level of the x-ray maps in alternative positions (*crossed circles*, Fig. 4). These three alternative sites corresponded to the three fully occupied sites that were assigned in the 1968x-ray model (Lenhert, 1968), in which the amide group occupies the N640 position. Thus, at least two alternative hydrogen bonding networks were found to be present in this region: (*a*) involving N40 and waters 211 and 212, and (*b*) involving N640 (or N840/1/2) and waters 601, 603, and 604.

Initially, the neutron density in this region was difficult

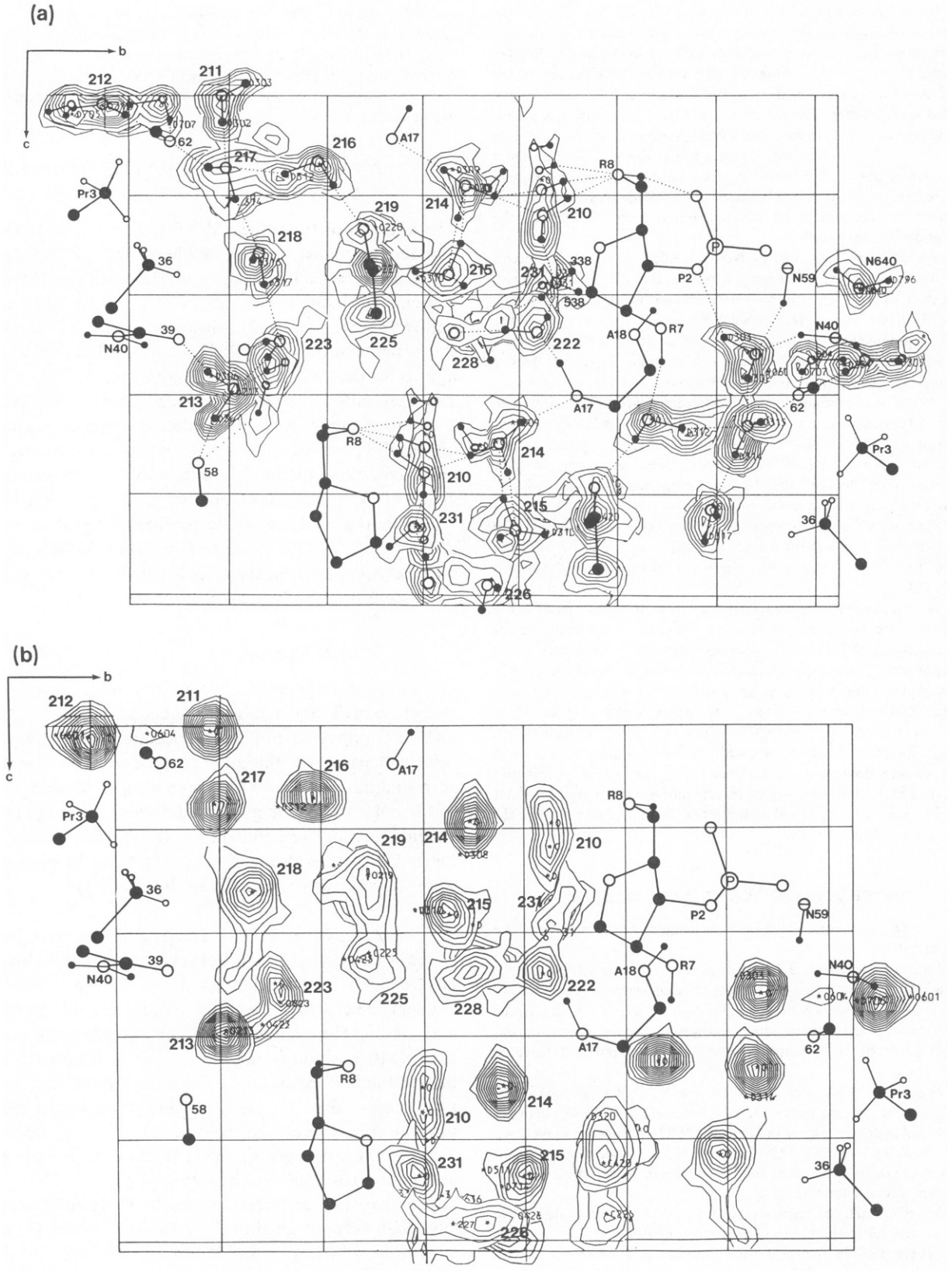

FIGURE 3 Summary of the "main" solvent density from $F_o - F_c$ difference Fourier syntheses using phases based on the coenzyme molecule. Two asymmetric units between the limits of $x = 0$ and $x = 1/2$ are projected onto the bc plane of the unit cell, over which a 3.0 Å grid is drawn: the outer edges represent the unit cell axes b and c. The atom code is given in the legend of Fig. 1. (*a*) Neutron: contour interval (ρ) = 0.015×10^{-12} cm, starting at the 0.030×10^{-12} cm level; $\sigma(\rho)$ ~0.02×10^{-12} cm. (*b*) X-ray2: contour interval (ρ) = 0.1e Å^3, starting at the 0.2 eÅ^{-3} level; $\sigma(\rho)$ ~0.15 eÅ^{-3}.

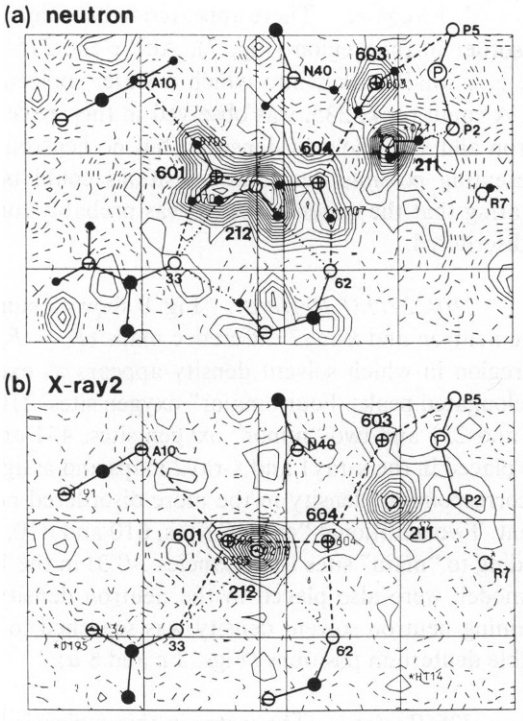

FIGURE 4 Solvent density (in the *ab* plane) around the disordered *c* side chain (N40) of the coenzyme molecule: (*a*) neutron and (*b*) x-ray2 $F_o - F_c$ difference Fourier syntheses using phases based on the coenzyme molecule. The contour intervals are: neutron = 0.01×10^{-12} cm, x-ray = 0.1 eÅ^{-3}; the atom code is given in the legend of Fig. 1. The disordered N640 position is not shown, but is located ~1.8 Å behind N40. Two independently, partially occupied solvent networks are present. Network *A* consists of waters 211 and 212, with occupancies of 0.9 and 0.6 in the x-ray2 and neutron models, respectively. Network *E* consists of waters 601, 603, and 604, with occupancies of 0.1 and 0.4 in the x-ray2 and neutron models, respectively.

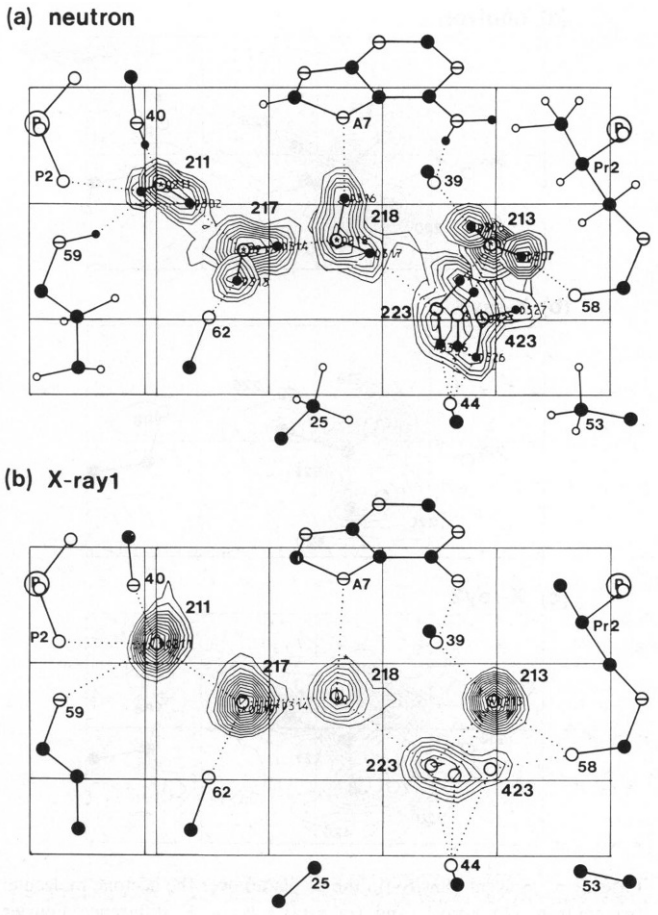

FIGURE 5 Summary of the solvent density over the 211, 217, 218, 223, and 213 regions projected onto the *ac* plane: (*a*) neutron, and (*b*) x-ray2 $F_o - F_c$ difference Fourier syntheses using phases based on the coenzyme molecule. The atom code and contour levels are given in the legends of Figs. 1 and 3, respectively.

to interpret without the aid of the x-ray models. The two "major" sites 211 and 212 were evident, but they were surrounded by six or seven other peaks, suggesting that their deuteriums could possibly be disordered. However, the three alternative "minor" oxygen sites of the x-ray models ("major" sites in the 1968x-ray model) were observed to correspond to three of the possible deuterium sites in the neutron map and it became very clear where the respective deuteriums for these "minor" sites were located (Fig. 4). The "minor" sites in the neutron model were seen to have higher occupancies (~0.4) than in the x-ray1 and x-ray2 models (~0.1).

216/217 Regions. The main solvent density peaks were elongated, especially around 217.

218/223/213 Regions. Fig. 5 shows composite difference syntheses of the solvent density in the 211, 217, 218, 223, and 213 regions. Deuteriums were clearly identified for the "main" oxygen sites 213 and 218. The 223 region, lying almost underneath the 213 water site, was seen to be disordered. From the x-ray1 and x-ray2 models, three water oxygen sites were assigned to the central region of the neutron density over 223 and six deuterium sites were placed in geometrically reasonable positions in the remaining neutron solvent density.

Location of the Acetone Molecule

Within the mouth of the pocket, five "main" solvent sites were assigned, 219, 220, 420, 221, and 225, which appeared to be in a plane and almost parallel to the plane of the benzimidazole base. When these sites were regarded as water oxygen sites, no sensible hydrogen bonded networks could be formulated that extended from the 219 and 220 positions to either the channel or the 218/223 regions (see Fig. 3).

The five sites were present in the same relative positions in the x-ray1, x-ray2, and neutron difference maps (Fig. 6) and four of these (219, 221, 420, and 225) were observed to have an acceptable geometry characterizing an acetone molecule. The proposed oxygen position, 219, had an expected higher peak height than the three carbon positions, 221, 420, and 225 in the x-ray maps, while in the neutron case the oxygen peak height was found to be lower.

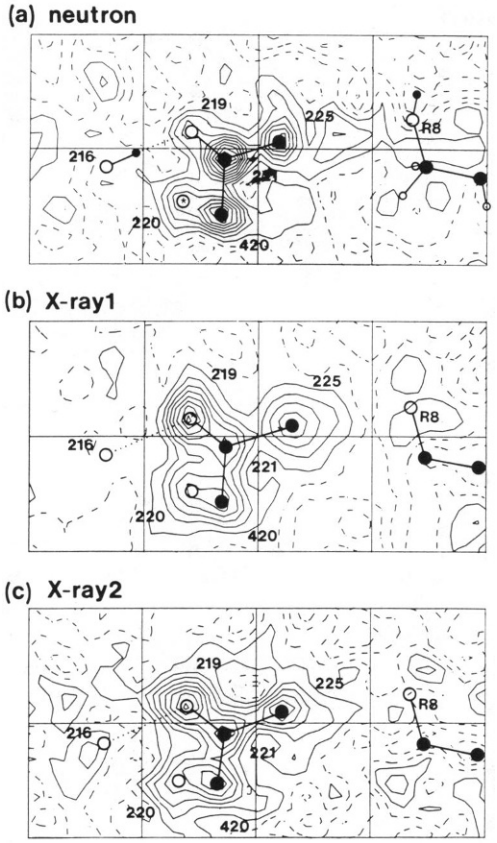

FIGURE 6 Solvent density (in the *ac* plane) over the acetone molecule: (*a*) neutron, (*b*) x-ray1, and (*c*) x-ray2 $F_o - F_c$ difference Fourier syntheses using phases based on the coenzyme molecule. The atom code and contour levels are given in the legends of Figs. 1 and 3, respectively.

Additional support for the assignment of an acetone molecule was gained from the observation that there were no prominent solvent sites of <3.4 Å from the two methyl groups C420 and C225. The fifth solvent site, 220, located near the C420 site was assigned as a disordered water site.

Channel Region

Eleven "major" solvent sites were initially observed in the x-ray1 and x-ray2 difference maps: 210, 410, 214, 215, 222, 226, 227, 228, 428, 231, and 235 (Fig. 3). Seven of these sites (410, 214, 215, 222, 226, 228, and 231) formed a reasonable hydrogen bonded network of water molecules with distances in the range of 2.5–3.2 Å. The neutron solvent density in the channel region appeared from the outset to be much more difficult to analyze than the x-ray solvent. Seven major regions of the solvent density could be localized that corresponded to the seven "main" oxygen solvent sites in the x-ray1 and x-ray2 models.

214 Region. Some elongated density was situated around the main peak(s).

215 Region. There appeared to be a high degree of disorder in this region (Fig. 7). Above the 215 region there is a small pocket into which a water molecule can pass. A small peak, 235, was observed in this space in the neutron and x-ray solvent densities, but no neutron peaks representing possible deuterium positions could be seen indicating that the water molecule was probably rotationally disordered.

210/222/231 Regions. Fig. 8 shows a summary of the neutron and x-ray2 difference maps ($F_o - F_c$) over this region in which solvent density appears as extended and elongated peaks. Four "major" oxygen sites, 210, 410, 222, and 231 and two "minor" oxygen sites, 431 and 831 were placed in the x-ray1 and x-ray2 maps and assigned to the corresponding density in the more disordered neutron solvent. Two additional "minor" sites, 610 and 810, corresponding to "main" sites (occupancies >0.3) in the 1968x-ray model, were also placed in the neutron density. The remaining neutron solvent density was searched to locate possible deuterium positions (Figs. 3 *a* and 8 *a*).

226 Region. The water in this region is hydrogen bonded to carbonyl O51 and the water oxygen appears to be more disordered than the deuterium H-bonding to O51 (Fig. 9).

228 Region. This was seen to be one of the most disordered solvent regions in the crystal, probably because the majority of the surrounding coenzyme groups were apolar.

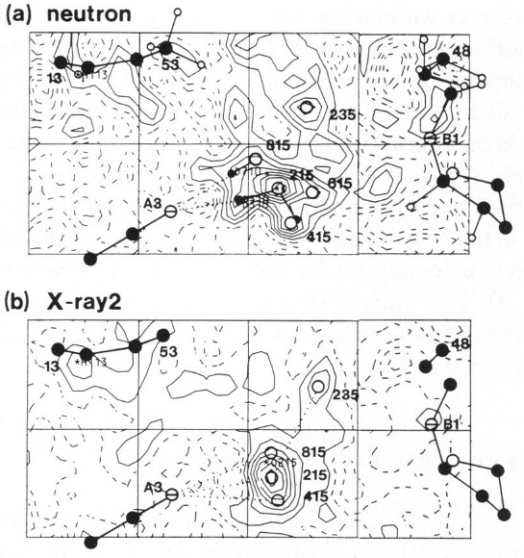

FIGURE 7 Solvent density (in the *ab* plane) over the 215 region: (*a*) neutron and (*b*) x-ray2 $F_o - F_c$ difference Fourier syntheses using phases based on the coenzyme molecule. The atom code and contour levels are given in the legends of Figs. 1 and 3, respectively.

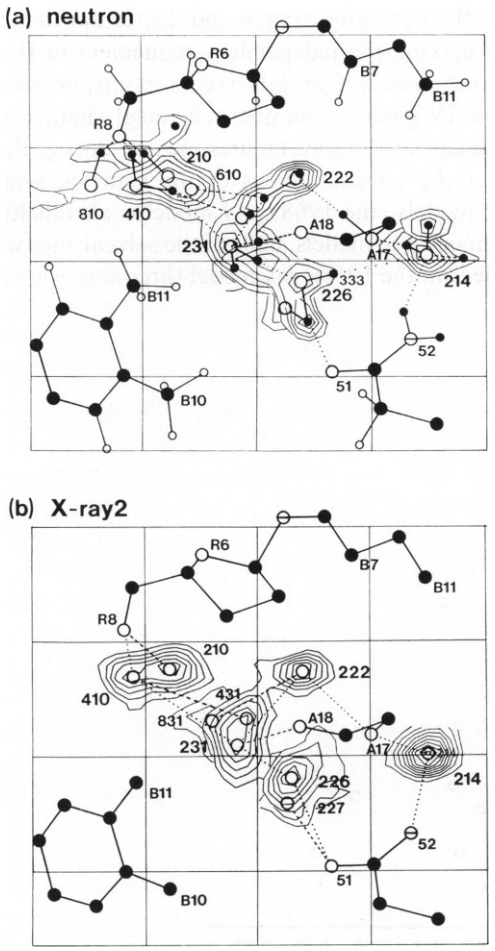

FIGURE 8 Summary of the solvent density over the 210/222/231 regions projected onto the *ac* plane: (*a*) neutron and (*b*) x-ray2 $F_o - F_c$ difference Fourier syntheses using phases based on the coenzyme molecule. The atom code and contour levels are given in the legends of Figs. 1 and 3, respectively. Dotted lines represent one H-bonding network; dashed lines represent alternative H-bonds.

Least-squares Refinement

In the above analysis the occupancies of the solvent sites were assigned from their relative peak heights in the map. Each site was then included in the respective model and their positional and thermal parameters (except for overlapping sites, <0.9 Å, in the neutron model) were allowed to vary in the least-squares refinement.

To try to obtain a better estimate of the occupancy parameters, these were also refined in separate cycles of least-squares refinement of the x-ray1 and x-ray2 models. For each model four cycles of refinement were carried out in which the positional, thermal, and occupancy parameters for each solvent site were varied simultaneously. None of the coenzyme parameters included in the structure factor calculation were varied during the occupancy refinement.

Although the thermal and occupancy parameters are known to be highly correlated in least-squares refinement, some encouraging results were observed for the more ordered solvent sites. For example, in the x-ray1 model the occupancy of the O213 and O423 sites, which were ~2.1 Å apart, adjusted to values of 0.77 and 0.23 after the third cycle with sensible temperature factors of $\overline{U} = 0.054$ and 0.075 Å^2, respectively, that were similar to the temperature factors of the surrounding coenzyme B_{12} atoms.

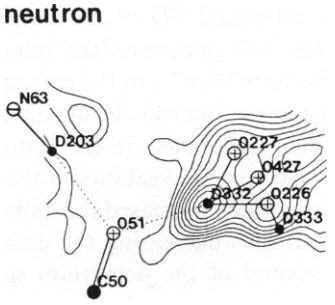

FIGURE 9 Neutron solvent density over the 226 region: $F_o - F_c$ difference Fourier synthesis using phases based on the coenzyme molecule. "Main" sites: 226 and 227; "continuous" site: 427. The atom code and contour levels are given in the legends of Figs. 1 and 3, respectively.

Where the solvent peaks overlapped, two different effects were evident. Whenever sites (~1.0 Å apart) were likely to be statically disordered, for instance in solvent regions well populated with polar groups such as the 212/601 region (Fig. 4 *b*), then the thermal and occupancy parameters for each site appeared to be well behaved. But where dynamic disorder was expected in regions containing few polar groups, for example in the 215/415 region (Fig. 7 *b*), the parameters had unrealistic values. Of the 42 solvent sites refined in the x-ray1 model, 31 were seen to have reasonably well behaved normal thermal and occupancy parameters, and were not seen to vary by more than twice their estimated standard deviations. The average estimated SD of the 31 occupancy parameters was ~0.05. The occupancies of these sites were then fixed to their refined values.

TABLE IV
NUMBER AND OCCUPANCY TOTALS OF THE SOLVENT SITES IN THE FOUR COENZYME MODELS AFTER THE FIRST SOLVENT ANALYSIS

	Neutron	X-ray1	X-ray2	1968x-ray
Number of sites				
Oxygens	47	54	52	38
Carbons	3	3	3	—
Deuteriums	52	—	—	—
Unknowns	7	—	—	—
Total	109	57	55	38
Sum of occupancies				
Oxygens and carbons	16.2	18.2	18.0	13.1
Deuteriums	17.5	—	—	—
Unknowns	1.3	—	—	—

The average estimated SD of the occupancies in the x-ray2 model was ~0.1 and the refined values for the main sites were seen to be within 2 σ of the corresponding values obtained for the x-ray1 model. Refinement of the occupancy and thermal parameters in the neutron model was not attempted, since (*a*) the visibility of the deuteriums in the neutron maps greatly increased the number of parameters to be refined, thus decreasing the data to parameter ratio, and (*b*) several of the deuterium sites overlapped with both alternative oxygen and deuterium sites (<0.9 Å apart) making the independent refinement of these sites, without the use of restraints or constraints, impossible.

Table IV gives the number, chemical identity and total occupancies of the solvent sites located during the refinement of the solvent regions of the neutron, x-ray1, and x-ray2 models (the 1968x-ray model is also included). In the former three models, none of the solvent sites were fully occupied. In the 1968x-ray model three sites were assigned

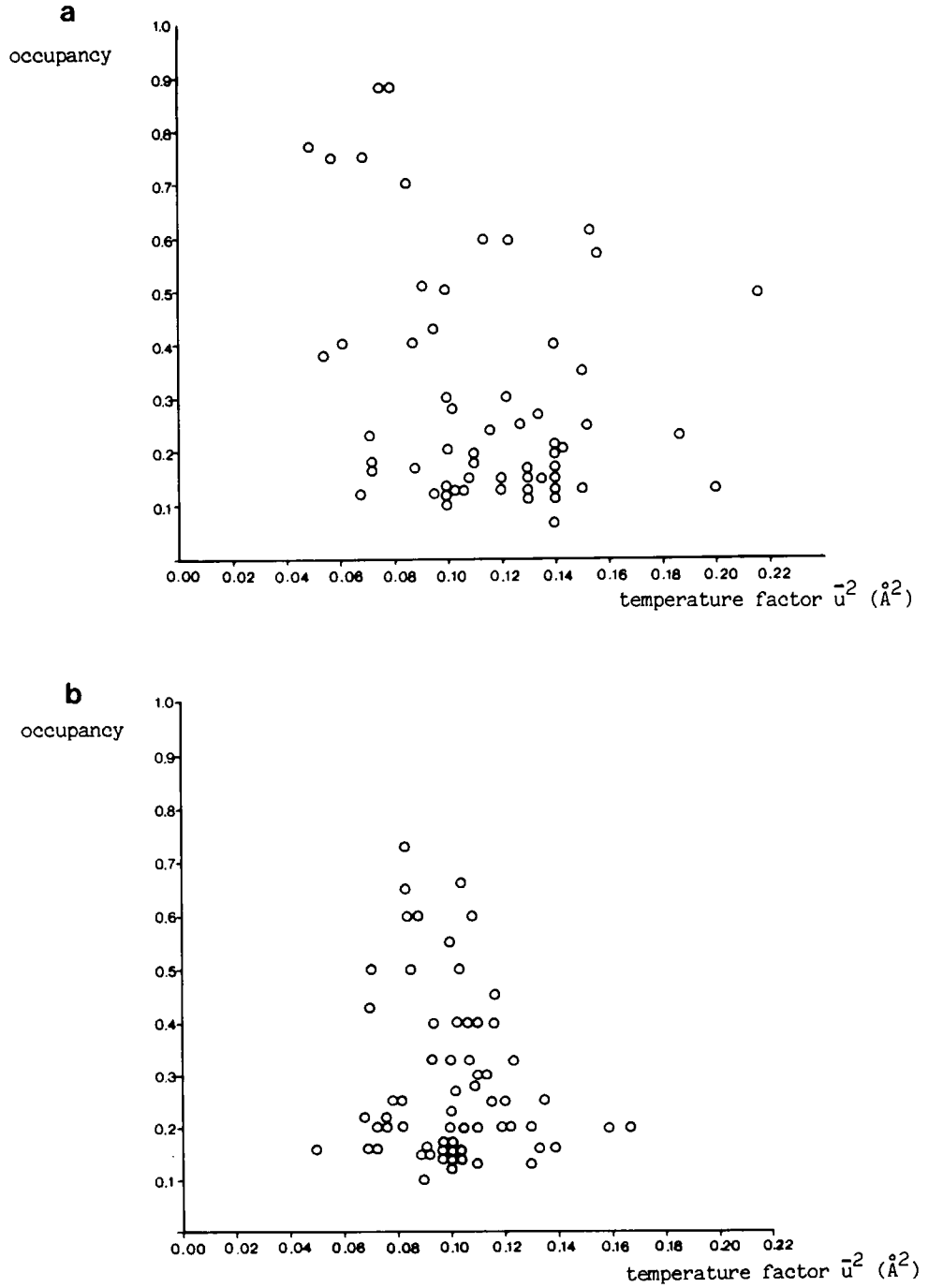

FIGURE 10 Plots of the solvent occupancy values against their respective temperature factors for (*a*) the x-ray2 model and (*b*) the neutron model.

full occupancies. However, a recent re-examination of the solvent density revealed that the peaks over these three sites are very much elongated indicating that the assigned sites are probably partially occupied. Plots of the occupancy values against the temperature factor values in (*a*) the x-ray1, and (*b*) the neutron models are given in Fig. 10. No clear correlation can be seen between the two parameters as many of the sites possess low occupancies of between 0.1 and 0.5 yet they have a wide range of temperature factors. In the majority of the solvent analyses performed on protein crystals, there appears to be a correlation between the occupancy factors and the temperature factors of the water sites: as the occupancy values decrease, the thermal factors increase. However, this may not be strictly correct, since possible ordered water sites with low occupanices and temperature factors on the surface of the protein may not be visible above the higher background levels found in most protein density maps. In the coenzyme B_{12} analysis, many of the waters with low occupancy values and attached to surface polar atoms, also possessed low thermal factors similar to those of highly occupied sites nearby. In addition to this, the thermal factors of the lower occupied waters further away from the coenzyme atoms tended to increase. Thus it may be more meaningful in the case of proteins, and other large solvated systems, to look at increases in the thermal factors with respect to the distance from the surface of the molecule.

WATER NETWORKS

Employing the criteria outlined in the Methods section, several alternative networks were derived from the partially occupied solvent sites of each of the models. These water networks extend throughout all the solvent regions of the crystal, and can be grouped into two major categories: one that includes the presence of the acetone molecule and one that does not. The acetone molecule, which is situated in the mouth of the pocket, effectively isolates the water molecules in the pocket region from those of the channel region. The networks are seen to be divided further into subgroups of networks associated with each of the two regions. Additional subdivisions also arise in the pocket region due to the disorder of the *c* side chain between two main positions for the nitrogen, N40 and N640.

Table V lists the labels and average occupancies assigned to the individual networks in the four different models. The water networks of the 1968x-ray model were not worked out in the original refinement of this model (Lenhert, 1968) and those given here, were derived from the 38 water sites included in the model.

The individual sites and their relative positions within the different water networks obtained from the four models, are illustrated in Fig. 11. Within each asymmetric unit of the neutron, x-ray1 and x-ray2 models, the main solvent networks *A*, *B*, and *C* (Table V) include the acetone molecule and ~14 water molecules. When the acetone is not present, then up to a maximum of ~17 or 18 water

TABLE V
SUMMARY OF THE SOLVENT NETWORKS FOR THE FOUR COENZYME B_{12} MODELS: LABELS AND ASSIGNED OCCUPANCIES OF THE INDIVIDUAL NETWORKS WITHIN EACH MODEL

Models	Pocket position of *C* side chain		Channel
X-ray 1 and X-ray 2	N40 (90%)	N840 (10%)	
(1) Acetone (60%)	A (60%)	—	B (40%)
			C (30%)
(2) No acetone (40%)	D (30%)	E (10%)	H (20%)
			I (10%)
		N640 (20%)	
Neutron	N40 (60%)	N840/1/2 (20%)	
(1) Acetone (50%)	A (50%)	—	B (35%)
			C (25%)
(2) No acetone (50%)	D (10%)	E (30%)	H, I etc
		F (10%)	
1968x-ray	N40 (0%)	N640/840 (100%)	
(2) No acetone (100%)	—	E (40%)	J (30%)
		F (20%)	I (15%)
		G (20%)	

molecules (from density measurements) can occupy each asymmetric unit. This latter arrangement represents the main water networks of the 1968x-ray model (in which no acetone molecule was located) and the more disordered water networks of the neutron, x-ray1, and x-ray2 models: *D–J*.

Acetone Molecule Present: Networks *A*, *B*, and *C*

The occupancy of the acetone molecule was estimated to be ~0.6 in the x-ray1 and x-ray2 models and ~0.5 in the neutron model. When this species is present, there appears to be one main water network in the pocket region (Network *A*) and two main water networks in the channel region (Networks *B* and *C*) (Figs. 11 *a* and *b*). These networks fill almost all of the accessible solvent space in the crystal except for three or four regions (see below) in which there exists spare space, but not enough to fit an additional water molecule into. These regions were seen to be close to apolar groups belonging to the coenzyme B_{12} molecule.

Network *A* consists of seven well defined water sites with occupancy values (in the neutron model) varying between 0.3(W223) and 0.7(W213). Thus several of these sites are also present in some of the other more disordered networks, particularly when the acetone is not present. For each of the seven oxygen sites, two ordered deuterium sites were observed in their expected positions, forming a complete hydrogen bonded network of waters throughout the pocket region. The O...O,N hydrogen bond distances vary from 2.6 to 3.2 Å, while the X-D...Y angles range from 130° to 174°. Water 212 appears to be isolated from any direct interactions with the other water molecules. Water 213 is strongly bound to the two carbonyls O39 and O58,

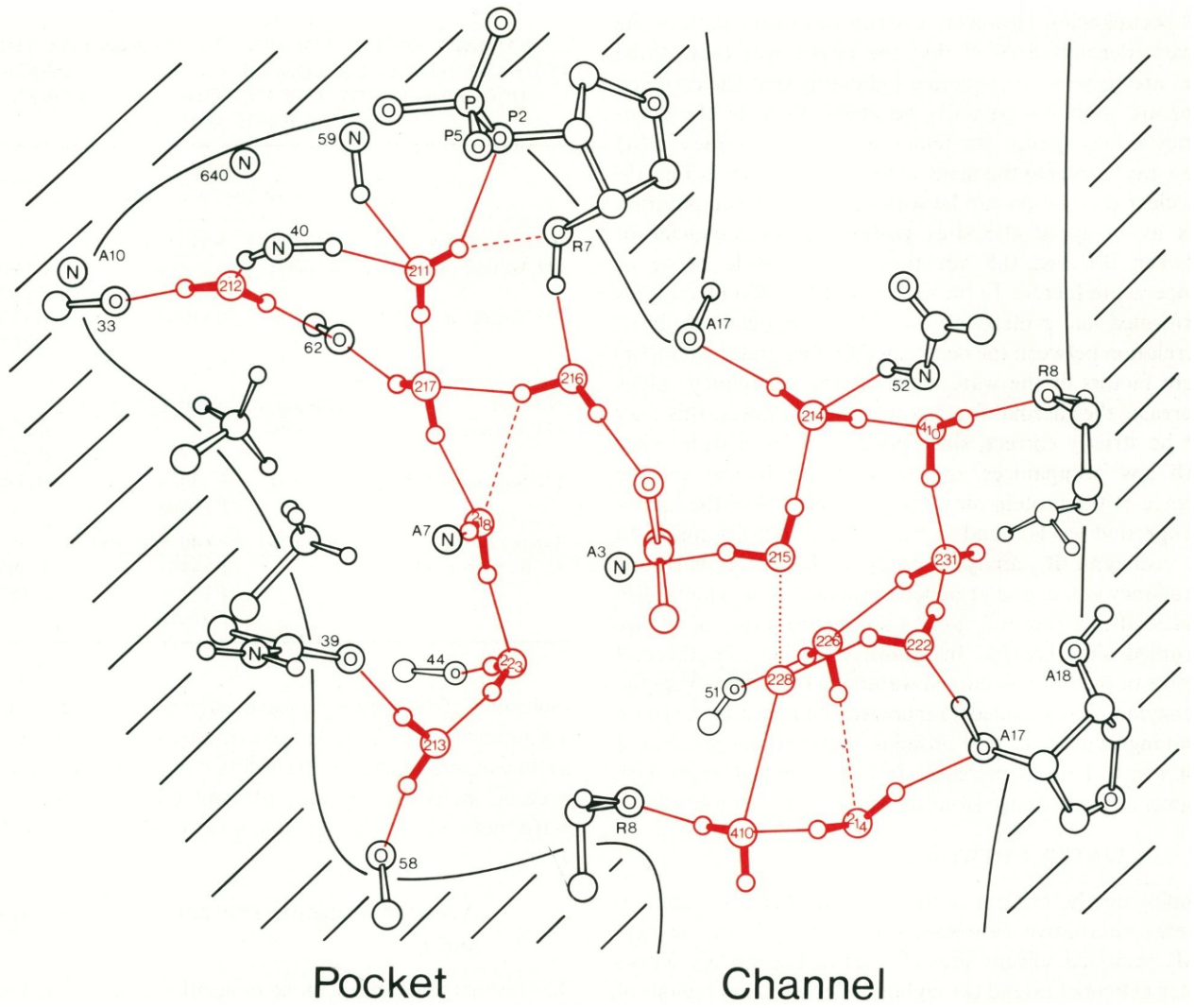

FIGURE 11 Water networks formulated from the solvent sites of the neutron, x-ray1, x-ray2, and 1968x-ray models. The networks for one asymmetric unit are drawn in projection onto the *bc* plane of the unit cell.

Network Colors:	Red	Blue	Yellow	Green	Purple	Orange
Pocket	A	A(v)	D	E	F	G
Channel	B	C	H	J	I	—

Networks included within Fig. 11:	(*a*)	(*b*)	(*c*)	(*d*)	(*e*)	(*f*)
Pocket	A	A,A(v)	A,D	A,E	A,E,F,G	All
Channel	B	B,C	B,H	B,J	B,I,J	All

A(*v*): variations of Network *A*. The hatched areas represent regions where coenzyme molecules lie. Fig. 11 *a* shown here.

while water 216 forms H-bonds to OR7, water 217, and oxygen 219 of the acetone. The three remaining water sites 217, 218, and 223 form a bridge between the top (phosphate region) and the bottom left-hand side (213 region) of the pocket (Figs. 3 and 5) passing between the CH_2 and CH_3 groups (C20, C25, C31, C35, and C36) of the coenzyme and methyls C225 and C420 of the acetone. No obvious alternative deuterium positions (>1.0 Å apart) were observed for these seven water sites. However, both the neutron and x-ray densities over these sites (and also the acetone molecule) are elongated in certain directions, indicating that they are probably disordered. Several alternative sites were assigned to these regions : 411(211), 416(216), 417(217), 418(218), and 623(223), [Network *A*(*v*)], which may well correspond to local movements of the waters within the network.

Network *B* consists of seven water oxygen sites and twelve deuterium sites, two each for six of the waters. These six waters form one or more hydrogen bonds to the polar atoms of the coenzyme molecule. The seventh water

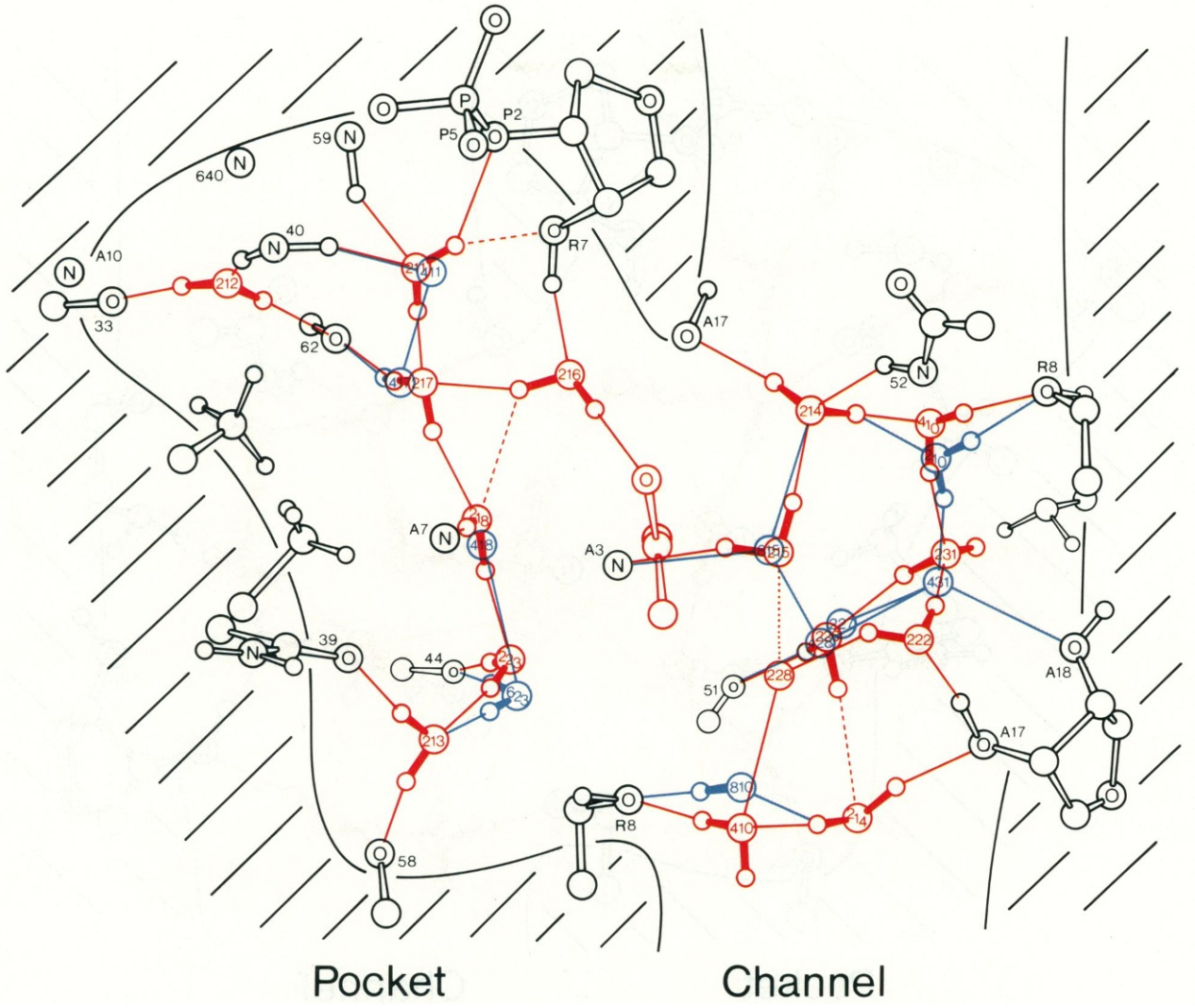

FIG. 11 *b*

228, is located in a very disordered region of the channel and forms hydrogen bonds only with surrounding water sites. All the deuteriums were seen to hydrogen bond to O and N acceptors apart from two: (*a*) One of the deuteriums of water 231 appeared to point toward the hydrogens of the C26 methylene group. The O231...C26 distance is ~3.3 Å and the (O231)-D338...H116-(C26) deuterium-hydrogen distance is 2.2 Å. There is an alternative position for D338 of 231, but it is less than the van der Waals D...D contact distance of ~2.0 Å from the deuterium of water 222 that forms a hydrogen bond to water 231. (*b*) Deuterium D333 of water 226 points toward the 214 water oxygen with a D...O distance of 2.5 Å, which is just above the accepted limit of ~2.4 Å for weak hydrogen bonding (Hamilton and Ibers, 1968).

Network *C* consists of six or seven water oxygen sites of which five form at least one hydrogen bond to the coenzyme polar groups. The water site O428 only forms hydrogen bonds to other waters. The possible seventh member of this network, the 235 site, is located in a large void above the 215 water position. Only eight deuterium sites were located in their expected linear positions (i.e., angles O-D...X = 150°–180°) for this network.

No Acetone Molecule Present: Networks *D–J*

Most of these networks occur in all four models. In the neutron, x-ray1 and x-ray2 models, fragments of various networks with low occupancies were formulated from the minor sites and some of the more highly occupied major sites (occupancies greater than networks *A*, *B*, and *C*). Two of these networks, *E* and *J*, correspond to the main networks of the 1968x-ray model in which they occur as major sites.

When the acetone molecule is not present, no well defined water networks can be formulated over the region that extends from the 223 region to the mouth of the pocket (where the acetone was located) and through to the 228 region of the channel (Fig. 3). There are probably two

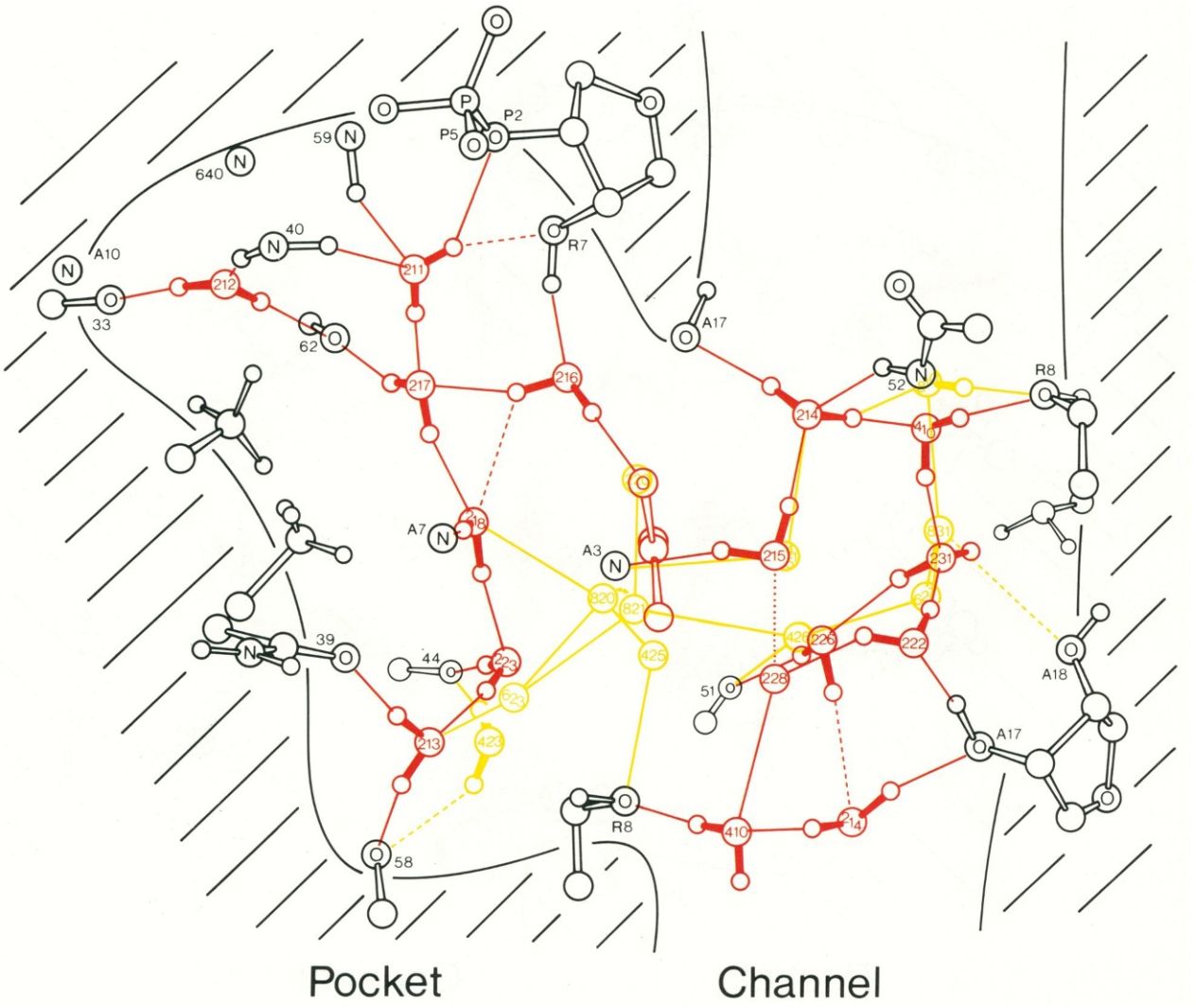

FIG. 11 *c*

main reasons for the disorder in this region. First, there is only one accessible polar group in this region, the OR8 hydroxyl, amongst the several apolar CH, CH_2, and CH_3 groups and the two base groups that are present. Second, movement of waters through the channel appears to be correlated with the disorder in the regions of the 215, 228, and 210 sites that are located around the mouth of the pocket.

Network *D* (pocket) is an extension of network *A* when the acetone molecule is absent. Four of the main sites 211, 212, 216, and 217 in network *A* are occupied and water 220 forms a hydrogen bond to 216 in place of the 219 oxygen of the acetone molecule. Eleven solvent sites with low occupancies (0.1 to 0.25) were assigned to the region extending from the 223 water site to the mouth of the pocket and several alternative networks can be chosen.

Network *E* (pocket) corresponds to the main water network of the 1968x-ray model, in which the three major sites, 601, 603, and 604, were assigned unit occupancies. The network breaks down in the mouth of the pocket (over the C225 area of the acetone), where again as with network *D* there are several alternative solvent sites with low occupanices.

Networks *F* and *G* (pocket) are some of the more incomplete alternative networks in the pocket region that extend from the 601, 603, and 604 sites.

Network *H* (channel) formulated starting from sites that were <3.5 Å from the methyl groups of the acetone molecule.

Networks *I* and *J* (channel) formulated from the sites in the channel region of the 1968x-ray model. The three sites, 214, 215, and 222, occupy the same relative positions as those in network *B*.

FURTHER ANALYSIS OF THE SOLVENT REGIONS: CONTINUOUS SITES

A second strategy was adopted to try to interpret the more diffuse, continuous and elongated regions of solvent density in terms of assigning "continuous sites" (see Methods). This was done only for the neutron solvent density, because

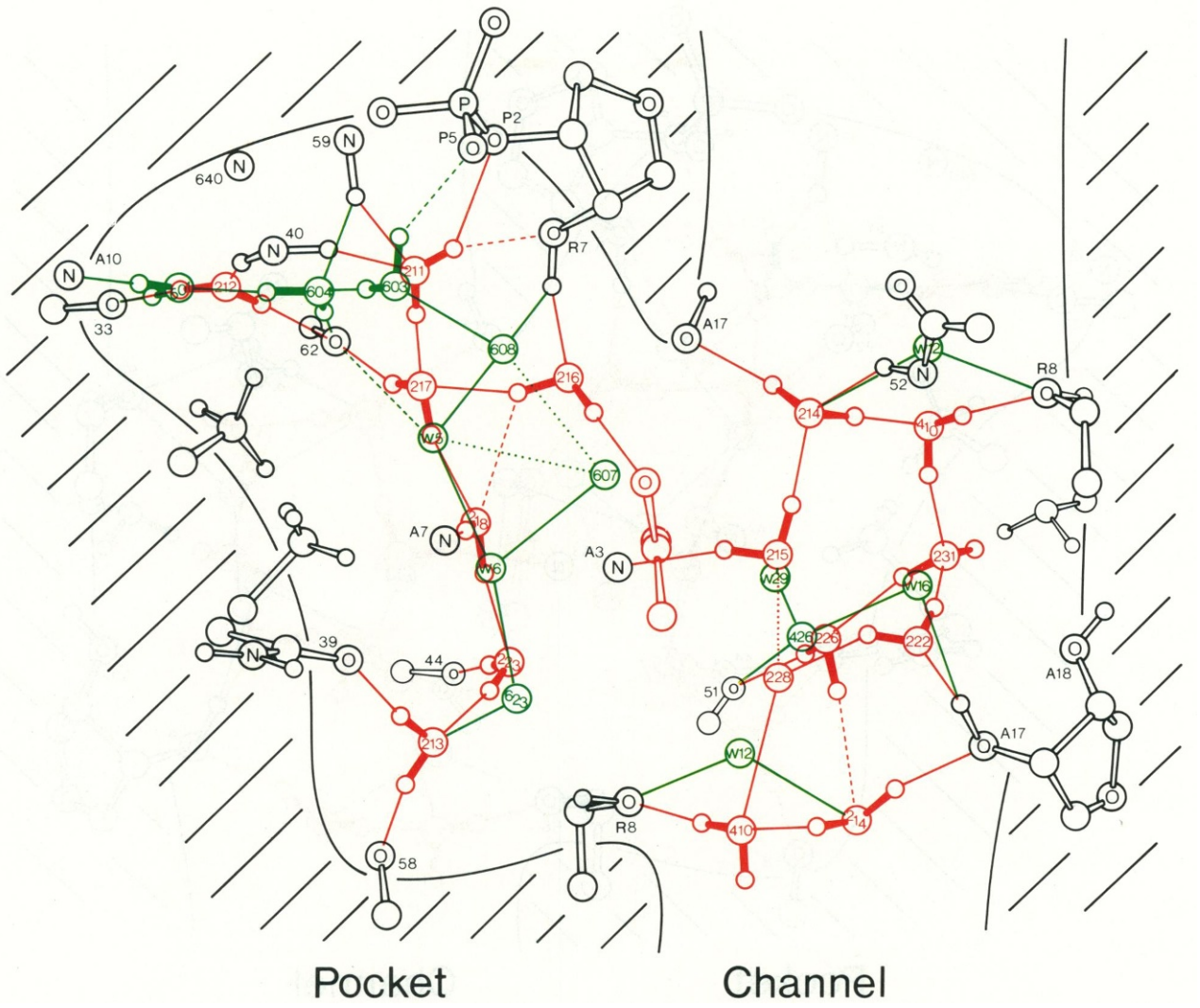

FIG. 11 *d*

from the first analysis only two reasonable networks of hydrogen bonded deuteriums were located, for networks *A* and *B*, despite the large number of assigned water oxygen networks in all four models. The total sum of the deuterium occupancies was ~19 (Table IV), but a sum of ~30 was expected for between 14 and 18 waters. This suggested that (*a*) the unobserved deuteriums may be too disordered to be clearly located in the solvent density, and/or (*b*) they may be in different positions than those expected for hydrogen bonding.

The geometries of the waters (and acetone) located in the first solvent analysis were regularized to the standard accepted values found in crystal hydrates: O-H = 0.96 Å and angle H-O-H = 107° (Chiari and Ferraris, 1982). Additional standardized waters (and acetone) were then assigned to the more diffuse regions of solvent density that were associated with possible disorder of the "main" sites. The new sites were placed at intervals of ~0.2–0.4 Å, that is, at approximately the resolution of the mean displacements of the refined temperature factors associated with the "main" sites. At present this is a very crude model and future improvements or the use of a more elaborate alternative model (such as a probability density) may subsequently be required to give a better description of the diffuse density. No attempt was made to refine the assigned "continuous" sites using least squares. However, their inclusion helped to identify some of the structural features of the possible water interactions such as the extent of the D...O distances of hydrogen bonds. In several cases, they were seen to range from ~1.6 to ~2.4 Å before the solvent density merged with the background level. Examples of some of the disordered regions are described below.

Pocket Region

Most of the "main" sites in Network *A* appeared to be associated with regions of surrounding elongated density. For example, three or four water positions could be placed in the extended density around water 211 (Fig. 12 *a*). Deuterium D303 of this water appears to be able to make

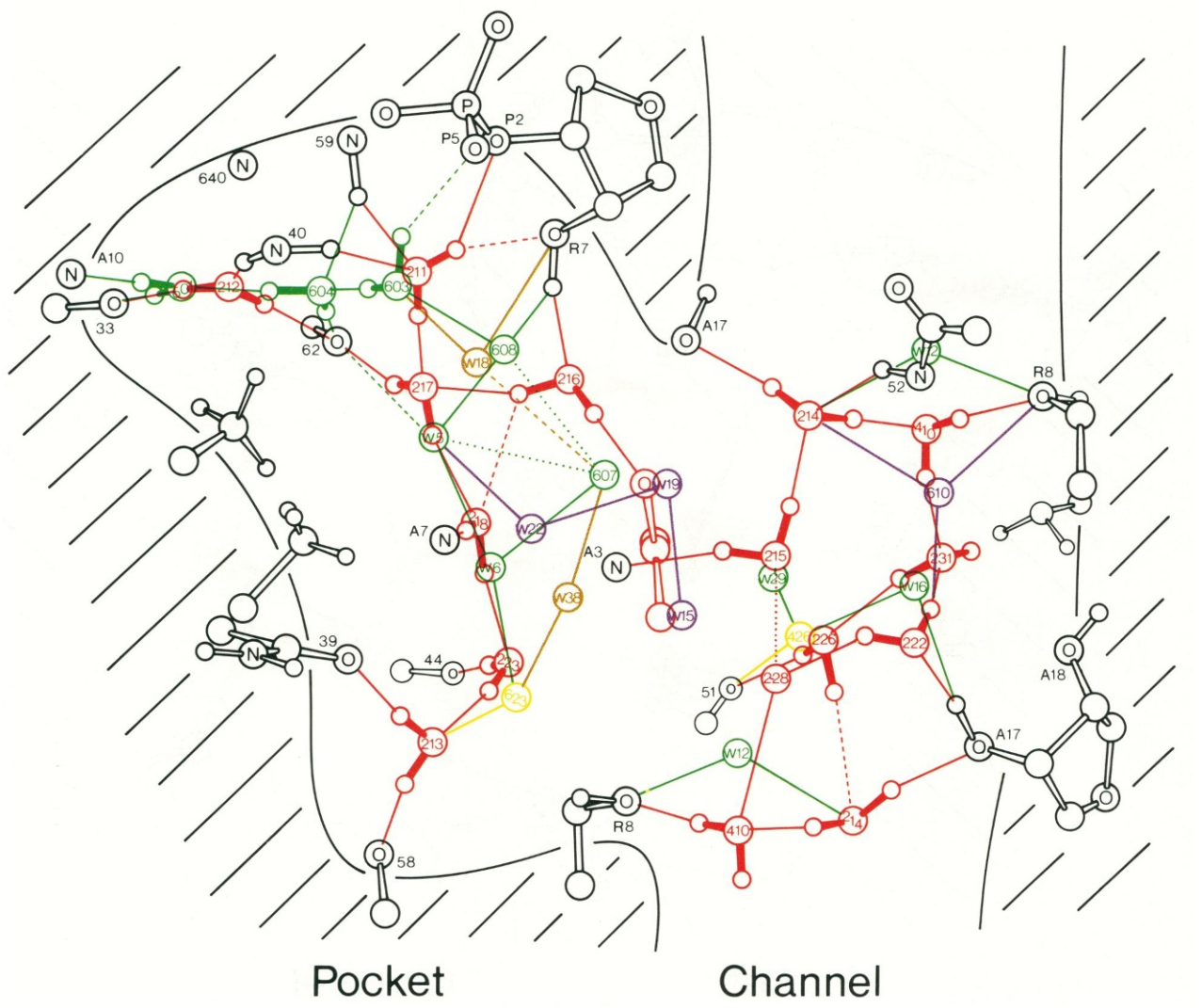

FIG. 11 *e*

alternate hydrogen bonds (and three centered ones) to both oxygens OP2 and OR7.

Channel Region

Extended neutron density was observed around water 214 (see Fig. 12 *b*) and four alternative water positions were placed within the density. The D...O distances of deuterium (D309) hydrogen bonding to the hydroxyl OA17 range from 1.9 to 2.3 Å and at the longer distance the neutron density over the deuterium was seen to fade away.

The water positions in the 210/410 region were seen to be greatly disordered around the hydroxyl oxygen OR8 situated on the edge of the pocket (Figs. 3 and 12 *c*). A continuous path of solvent density was observed alongside the OR8 oxygen extending down the *c* axis from one asymmetric unit to the next. In addition to the two major sites located (210 and 410) several others were included at intervals of ~0.3 Å (Fig. 12 *c*). There is extensive elongated density for the deuterium that H-bonds to OR8. It appears that a water can move in from the top (or the bottom) on the left-hand side of OR8 and initially form a weak H-bond (~2.3 Å) and then move into the 210/410 region where it forms a stronger H-bond (1.6–2.0 Å). From here it can move downward, weakening the bond to OR8 and then eventually break away (possibly pulled by another water) to move further down the channel.

All the remaining regions of solvent density were also observed to be disordered. Where the deuteriums appeared to be on the verge of severe disorder at the longer and weaker D...O distances of 2.1–2.4 Å or greater, it was almost impossible to form hydrogen bonding networks. Most of the less severe disorder of the water oxygens could be consistently traced in the four models, but the majority of their deuterium atoms were not visible in the neutron solvent density. With the inclusion of the "continuous" sites, a total of ~120 different water positions were assigned in the neutron model, of which over 90% were consistent with the other models.

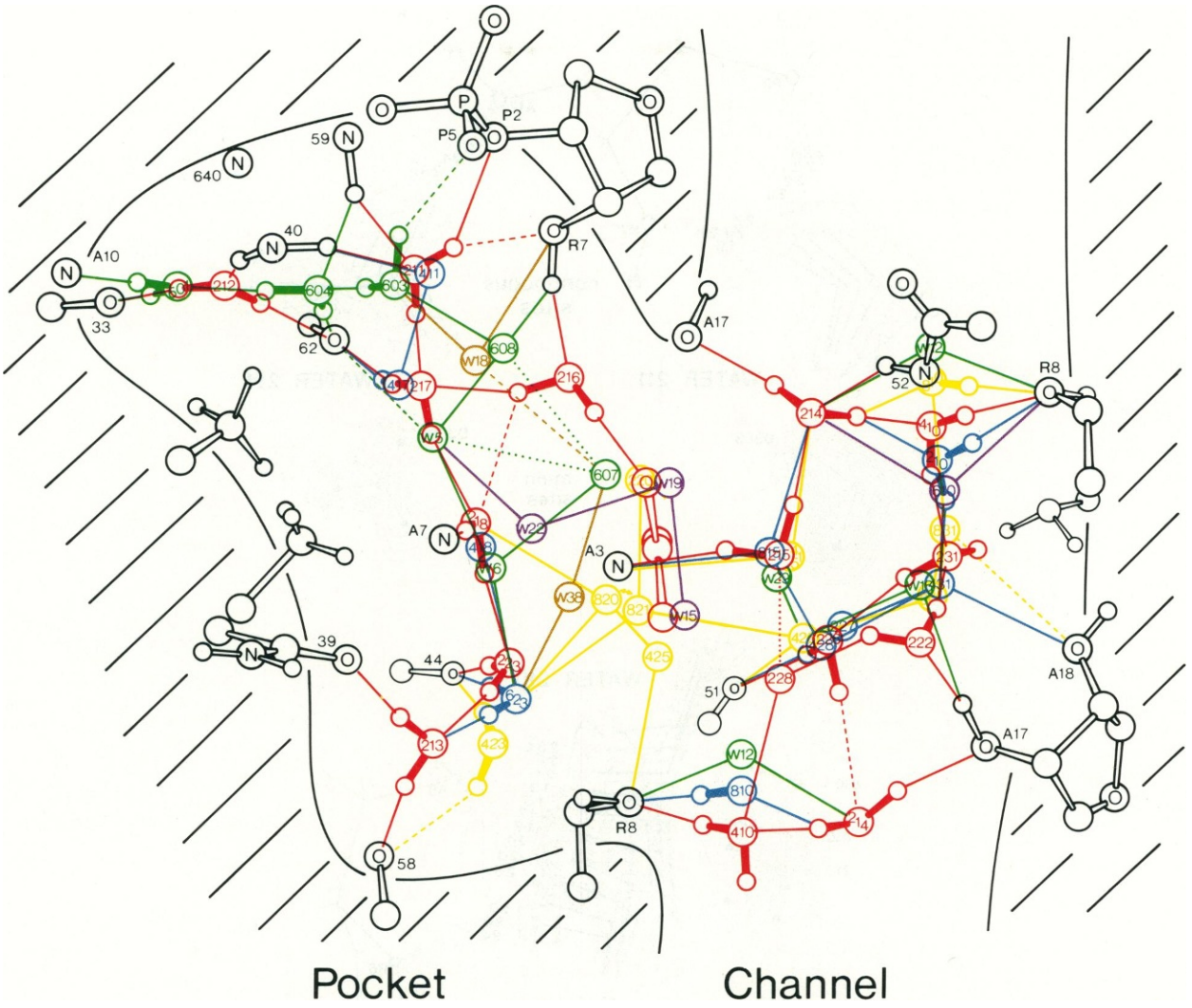

FIG. 11 *f*

DISCUSSION: CONSISTENCY OF THE WATER NETWORKS

To interpret the solvent density in the above two analyses, it was found necessary to place many of the water positions in regions of weak and diffuse density, some of which were near the noise level of the maps. The procedures used can be justified through the resulting self-consistency of the assigned sites between each of the four models (see section on Strategy of the Solvent Analysis, above). In such a highly disordered situation no other approach can be seen at present that would make use of all the available data and maintain sensible water molecule geometries.

In performing the whole analysis, it was necessary to use as much information as possible that could be gained from the different sets of diffraction data used: with only one set of (albeit neutron) data, it would have been almost impossible at this stage, to reach the same conclusions confidently. Combined and individual analyses of the models revealed many of the characteristics of the solvent structure. Specific networks were formulated (using criteria given in the Methods section) in each of the models and when present, the networks were seen to be consistent with those in the other models, in terms of the individual water sites occupying similar positions. However, the occupancies of the individual networks were frequently seen to have different values in each of the four models, sometimes being highly occupied in one model but barely visible in another, for example, network *E* in Fig. 4. This phenomona was probably due to the slightly differing physical conditions of the crystals that were used during the collection of the diffraction data. One parameter that was clearly seen to vary between the data sets was the temperature: from ~4° to 21°C (see Table I). This variation can explain in part the observed differences, among the four models, of the network occupancies with respect to the disorder of side groups (*c* side chain) and also a rearrangement of hydrogen bonds around the phosphate group (details given in

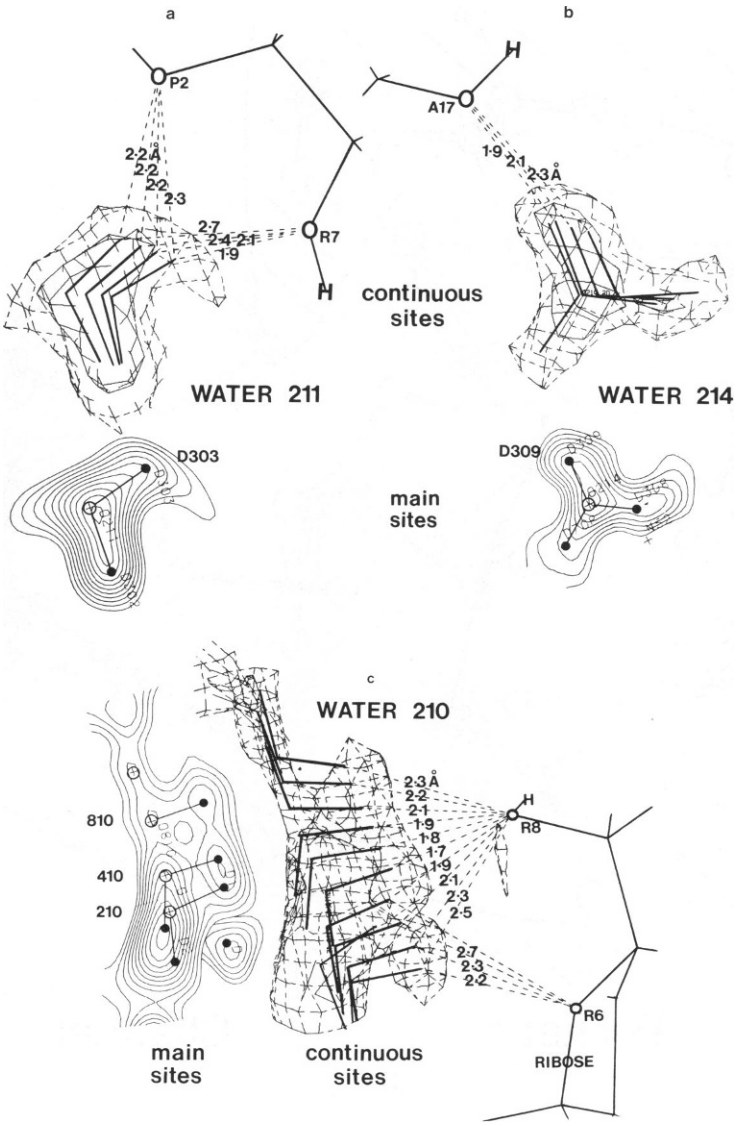

FIGURE 12 Interpretation of the solvent density over (*a*) the 211 region, (*b*) the 214 region, and (*c*) the 210 region. Main sites were initially assigned to the well defined solvent density. Continuous sites were assigned to the elongated and diffuse regions of solvent density.

Savage et al., 1986). Effects such as temperature deviation imply that small environmental changes can significantly perturb solvent organization, a point of relevance to the role of water in biomolecular processes (Finney, 1984).

With respect to both static and dynamic disorder, all of the water structure in the coenzyme crystal appears to be disordered. However, if well defined static disorder is classified as a form of partial order, then some of the water structure is ordered, particularly in the pocket region, while the remainder is disordered, especially in the channel. With the fractionally occupied acetone molecule present between the two solvent regions, one main water network in the pocket region and several consistent networks in the channel region were evident. In addition to these networks, local disorder around each of the main water sites was also observed. Table VI lists the mean positional deviations of the corresponding solvent oxygen and carbon (acetone molecule) sites located in the first solvent analysis among the neutron, x-ray1 and x-ray2 models. As expected there is better agreement between the corresponding solvent positions for the more ordered networks *A*, *B*, and *C* than for the disordered ones. The relatively low values of the RMS deviations (lower than generally achieved so far in comparing computer simulations with experiment; Vovelle et al., 1985) are very encouraging, and again give additional verification of the solvent interpretation.

The overall occupancy values assigned to the different networks obtained from the first solvent analysis are given in Table V. When the occupancies for the multiple water oxygen sites (sites which participate in more than one network) were summed, their values were within ~0.1 of

TABLE VI
POSITIONAL DEVIATIONS (IN ANGSTROM) OF THE CORRESPONDING NONDEUTERIUM SOLVENT SITES BETWEEN THE X-RAY1, X-RAY2, AND NEUTRON MODELS.

Models	Networks (number of sites in brackets)			
	A, B, C	*D–J*	All	Max
Neutron/x-ray1	0.23 (25)	0.39 (14)	0.27 (39)	0.70
Neutron/x-ray2	0.22 (25)	0.43 (14)	0.29 (39)	0.69
X-ray1/x-ray2	0.14 (25)	0.31 (27)	0.23 (52)	0.67

their values obtained from the refinement. However, these occupancies are probably overestimated for certain sites, since from the second analysis several additional sites were assigned to the adjacent regions, within 2.0 Å. Without the 1968x-ray model being available, the highly occupied networks *E*, *F*, and *J* (>0.3) in this model would have been very difficult to formulate with any certainty in the other three models, since within the latter models the networks appeared as disordered sites with relatively low occupancies, mainly <0.3.

Further discussions of the structural characteristics and details of the water-water and water-coenzyme interactions with respect to hydrogen bonding geometries, coordinations, nonbonded interactions contacts, water network bonding geometries, and orientational dependencies, are described in the second part of this article.

Thanks are due to John Allibon, John Finney, Mogens Lehmann, Peter Lindley, and Peter Timmins in the collection and processing of the neutron diffraction data. I am also indebted to John Finney for his continuous and informative advice throughout the course of this work.

Support from the Science and Engineering Research Council, United Kingdom and the National Institutes of Health, is gratefully acknowledged.

Received for publication 19 April 1985 and in final form 30 April 1986.

REFERENCES

Chiari, G., and G. Ferraris. 1982. The water molecule in crystalline hydrates studied by neutron diffraction. *Acta Crystallogr.* B38:2331–2341.

Cooke, R., and I. D. Kuntz. 1974. The properties of water in biological systems. *Annu. Rev. Biophys. Bioeng.* 3:95–126.

Edsall, J. T., and H. A. McKenzie. 1978. Water and proteins. I. The significance and structure of water; its interaction with electrolytes and nonelectrolytes. *Annu. Rev. Biophys. (Tokyo).* 10:137–207.

Edsall, J. T., and H. A. McKenzie. 1983. Water and proteins. II. The location and dynamics of water in protein systems and its relation to their stability and properties. *Annu. Rev. Biophys. (Tokyo).* 15:53–183.

Ferraris, G., and M. Franchini-Angela. 1972. Survey of the geometry and environment of water molecules in crystalline hydrates studied by neutron diffraction. *Acta Crystallogr.* B28:3572–3583.

Finney, J. L. 1977. The organisation and function of water in protein crystals. *Philos. Trans. R. Soc. Lond. B. Biol. Sci.* 278:3–32.

Finney, J. L. 1978. The organisation and function of water in protein crystals. *In* Water: A Comprehensive Treatise. F. Franks, editor. Plenum Publishing Corp., New York. 6:279–409.

Finney, J. L., J. M. Goodfellow, and P. L. Poole. 1982. The structure and dynamics of water in globular proteins. *In* Structural Molecular Biology. D. B. Davies, W. S. Saenger and S. S. Danyluk, editors. Plenum Publishing Corp., New York. 387–426.

Finney, J. L. 1984. Solvent effects in biomolecular systems and processes. *J. Phys. Colloque.* C7:197–210.

Finney, J. L., J. M. Goodfellow, P. L. Howell, and F. Vovelle. 1985. Computer simulation of aqueous biomolecular systems. *J. Biomol. Struct. & Dyn.* 3:599–622.

Hamilton, W. C., and J. A. Ibers. 1968. Hydrogen Bonding in Solids. The Benjamin Co., Inc., Elmsford, New York.

Kuntz, I. D., and W. Kauzman. 1973. Hydration of proteins and polypeptides. *Adv. Protein Chem.* 28:239–345.

Lenhert, P. G., and D. C. Hodgkin. 1961. Structure of the 5,6-dimethylbenzimidazolylcobamide coenzyme. *Nature (Lond.).* 192:937–938.

Lenhert, P. G. 1968. The structure of vitamin B_{12} VII. The x-ray analysis of the vitamin B_{12} coenzyme. *Proc. R. Soc. Lond. B. Biol. Sci.* A303:45–84.

Mason, S. A., G. A. Bentley, and G. J. McIntyre. 1984. Deuterium exchange in lysozyme at 1.4 Å resolution. *Basic Life Sci. Neutrons Biol.* 27:323–334.

Savage, H. F. J., and A. Wlodawer. 1986. Determination of water structure around biomolecules using x-ray and neutron diffraction methods. *Methods Enzymol. Biomembr.* 127:599–622.

Savage, H. F. J., J. L. Finney, P. F. Lindley, and P. A. Timmins. 1986. High resolution neutron and x-ray refinement of vitamin B_{12} coenzyme, $C_{72}H_{100}N_{18}O_{17}PCo.17H_2O$. *Acta Cryst. B.* In press.

Teeter, M. M., and A. A. Kossiakoff. 1984. The neutron structure of the hydrophobic plant protein crambin. *Basic Life Sci. Neutrons Biol.* 27:335–348.

Vovelle, F., J. M. Goodfellow, H. F. J. Savage, J. L. Finney, and P. Barnes. 1985. Solvent structure in vitamin B_{12} coenzyme crystals: computer simulation study. *Eur. Biophys. J.* 11:225–237.